Spermiogenesis Initiation in *Caenorhabditis elegans* Involves a Casein Kinase 1 Encoded by the *spe-6* Gene

Paul J. Muhlrad and Samuel Ward[1]

Department of Molecular and Cellular Biology, The University of Arizona, Tucson, Arizona 85721

Manuscript received December 7, 2001
Accepted for publication February 18, 2002

ABSTRACT

Immature spermatids from *Caenorhabditis elegans* are stimulated by an external activation signal to reorganize their membranes and cytoskeleton to form crawling spermatozoa. This rapid maturation, termed spermiogenesis, occurs without any new gene expression. To better understand this signal transduction pathway, we isolated suppressors of a mutation in the *spe-27* gene, which is part of the pathway. The suppressors bypass the requirement for *spe-27*, as well as three other genes that act in this pathway, *spe-8*, *spe-12*, and *spe-29*. Eighteen of the suppressor mutations are new alleles of *spe-6*, a previously identified gene required for an early stage of spermatogenesis. The original *spe-6* mutations are loss-of-function alleles that prevent major sperm protein (MSP) assembly in the fibrous bodies of spermatocytes and arrest development in meiosis. We have isolated the *spe-6* gene and find that it encodes a predicted protein-serine/threonine kinase in the casein kinase 1 family. The suppressor mutations appear to be reduction-of-function alleles. We propose a model whereby SPE-6, in addition to its early role in spermatocyte development, inhibits spermiogenesis until the activation signal is received. The activation signal is transduced through SPE-8, SPE-12, SPE-27, and SPE-29 to relieve SPE-6 repression, thus triggering the formation of crawling spermatozoa.

SPERM in the nematode *Caenorhabditis elegans* accumulate as immotile spherical spermatids, which are incompetent for fertilization. In response to extracellular signals, the cells undergo spermiogenesis, a rapid and dramatic morphological transformation to mature amoeboid spermatozoa, and immediately begin crawling. Because this maturation occurs without any new mRNA or protein synthesis, spermiogenesis initiation affords an opportunity to study a signaling pathway that acts post-translationally to regulate cellular morphogenesis in a genetically tractable organism. Moreover, nematode sperm provide a distinctive system for investigating the acquisition of cellular motility because they derive their crawling motility from an unconventional cytoskeleton containing neither actin filaments nor microtubules (reviewed in Roberts and Stewart 1995, 2000; Theriot 1996; Italiano *et al.* 2001).

As they develop, *C. elegans* sperm become streamlined toward their sole task of encountering and fertilizing oocytes. Spermatocytes, the progenitors of spermatids, are biosynthetically active cells, producing all the components that will be needed in the mature spermatozoa. One key component, which will form the cytoskeleton responsible for motility, is a small protein called major sperm protein (MSP). Spermatocytes synthesize large amounts of MSP and package it into paracrystalline arrays called fibrous bodies (FBs), which form a complex with novel structures termed membranous organelles (MOs). Each spermatocyte divides twice in meiosis and segregates a subset of its contents to the resulting four haploid spermatids. Each spermatid receives a nucleus, mitochondria, FB-MOs, and other molecular machinery necessary for forming a pseudopod, for crawling, and for fertilization. Components not needed in the spermatids, including ribosomes, endoplasmic reticulum, Golgi, and the actin and tubulin cytoskeletons, are jettisoned to an anucleate residual body and subsequently degraded. After spermatids detach from the residual body, the FBs disassemble and release their MSP to the cytosol, where it remains largely depolymerized until spermiogenesis commences.

Within minutes after exposure to the (as yet unidentified) spermiogenesis initiation signal, MOs fuse with the plasma membrane at one side of the cell. A pseudopod extends from the opposite side. MSP polymerizes within the pseudopod, forming a dynamic cytoskeleton that pushes the tip of the pseudopod forward while simultaneously drawing the cell body forward (Nelson and Ward 1980; Ward *et al.* 1983; Italiano *et al.* 2001).

Many mutants defective in sperm development have been isolated as self-sterile hermaphrodites that can be rescued by mating with wild-type males (Kimble and Ward 1988; L'Hernault 1997). Four such genes characterized in our laboratory—*spe-8*, *spe-12*, *spe-27*, and *spe-29*—are involved in transducing the signal that initiates spermiogenesis (L'Hernault *et al.* 1988; Shakes and Ward 1989; Minniti *et al.* 1996; Nance *et al.* 1999,

[1]*Corresponding author:* University of Arizona, Department of Molecular and Cellular Biology, 452 Life Sciences South, 1007 Lowell St., Tucson, AZ 85721. E-mail: samward@U.arizona.edu

2000). In this article, we report the isolation of new mutations that suppress mutations in all four of these spermiogenesis initiation genes. We show that 18 of these suppressor mutations are alleles of *spe-6*. We have identified the *spe-6* gene, which encodes a protein-serine/threonine kinase of the casein kinase 1 (CK1) family. Our results suggest that *spe-6*, which our laboratory previously found is necessary for MSP assembly and segregation of cellular components early in sperm development (Varkey *et al.* 1993), is also central to the signaling pathway that initiates spermiogenesis.

MATERIALS AND METHODS

Strains and general nematode methods: Standard methods for culture and genetic analysis of *C. elegans* were performed as described (Brenner 1974; Wood 1988; Lewis and Fleming 1995). Genetic nomenclature follows as described by Horvitz *et al.* (1979) and Hodgkin (1995). For temperature-sensitive strains the permissive temperature was 15° and the restrictive temperature was 25°. For some experiments, nematodes were reared at 20°. *C. elegans* N2 var. Bristol was the wild-type parent of all mutant strains. The following genes and mutations used are described by Riddle (1997) or in references therein: LGI: *spe-8(hc79)*, *spe-12(hc76)* (Nance *et al.* 1999), *dpy-5(e61)*, *fer-1 (hc13ts)*, *unc-29(e1072)*; LGIII: *dpy-1(e1)*, *dpy-18(e364)*, *spe-6 (hc49, hc92, hc143, hc146)*, *vab-7(e1562)*, *unc-25(e156)*; LGIV: *unc-22(e66)*, *dpy-20(e1282*ts), *spe-27(it132*ts, *it110, hc161)*, *spe-29 (it127)* (Nance *et al.* 2000); LGV: *him-5(e1490)*. The following chromosome III rearrangements and balancers were used: *qC1*, *tDf2*, *tDf7*, *ctDf3*, *ctDf2* and *eDp6* (Edgley *et al.* 1995).

Isolation of suppressor mutants: To isolate suppressors of the temperature-sensitive hermaphrodite-self-sterile phenotype imposed by *spe-27(it132)*, large populations of *spe-27(it132) unc-22(e66)* hermaphrodites were raised at the permissive temperature. The *unc-22* mutation was included in the strain to preclude mating by males in the population because *spe-27* mutant hermaphrodites are fertile when mated to males. *unc-22(e66)* males cannot copulate. The populations, which contained many L4 larvae and young adults, were mutagenized for 4 hr at 15° in 50 mM ethyl methanesulfonate (Sigma, St. Louis) as described by Anderson (1995), and the mutagenized worms were distributed among many bacteria-seeded nematode growth medium agar plates. The plates were incubated at 15° for approximately two generations so that recessive suppressors would be homozygous prior to selection at 25°. After shifting the populations to 25°, the worms were periodically transferred to fresh plates. The majority of worms died after several weeks, and most survivors produced no progeny due to their *spe-27(it132)* mutation, but some plates sustained populations. From each plate containing populations, we picked a single worm to a fresh plate and cultured it at 25° to establish independent suppressor lines. We estimate that the F_2 progeny of ~156,000 F_1 mutagenized individuals were subjected to selection in this screen.

Dominance and complementation tests between suppressor mutants: To test the suppressor mutants for dominance, young adult *spe-27(it132) unc-22(e66); "sup-X"* hermaphrodites were mated to *spe-27(it132)* males. F_1 cross-progeny hermaphrodites (*i.e.*, non-Unc) were scored for self-fertility at 25°. In almost every case, all the F_1 cross-progeny were sterile, indicating that the suppressor mutation was recessive. For two mutants, all or most of the F_1 cross-progeny were weakly self-fertile, indicating semidominance. Suppressor strains used in complementation tests were outcrossed at least twice to *spe-27(it132)* males to remove any secondary mutations. Outcrosses also indicated that the suppressor mutations are not true revertants of *spe-27(it132)* since the suppression phenotype always segregated independently from *unc-22(e66)*, which is itself closely linked to the *spe-27* mutation in the suppressor strains. For complementation tests *spe-27(it132) unc-22(e66)/+ +; "sup-X"/+* males were mated to *spe-27(it132) unc-22(e66); "sup-Y"* hermaphrodites. One-half of the outcross (*i.e.*, non-Unc) hermaphrodite progeny from this cross should be self-fertile if *sup-X* and *sup-Y* fail to complement; if the two mutants complement each other, no fertile cross-progeny are expected. All pairwise combinations of the five strongest suppressor mutants (*hc163*, *hc164*, *hc165*, *hc166*, and *hc167*) were tested for complementation. In addition, the strongest suppressing strain, *hc163*, was tested for complementation of the remaining nine strongest suppressing recessive mutants.

Testing suppression of null *spe-27* alleles and other spermiogenesis mutants: *spe-27(it132) unc-22(e66); hc163* hermaphrodites were crossed to *spe-27(it110) dpy-20(e1282)* males. F_1 male and hermaphrodite siblings were intercrossed, and their Dpy, non-Unc hermaphrodite progeny were scored for fertility at 25°. Similar crosses were performed to test *hc163* suppression of *spe-27(hc161)* (Minniti *et al.* 1996), *spe-12(hc76)* (Shakes and Ward 1989; Nance *et al.* 1999), and *spe-29(hc127)* (Nance *et al.* 2000). To test whether *hc163* suppresses *spe-8(hc79)*, *spe-27(it132); hc163 dpy-18(e364)* hermaphrodites were mated to *spe-8(hc79)* mutant males (*hc163* is closely linked to *dpy-18*). F_2 Dpy hermaphrodites were scored for self-fertility. Approximately three-fourths of the F_2 should be heterozygous for *spe-8(hc79)* or homozygous wild type and would be fertile. One-fourth should be homozygous for *spe-8(hc79)* and would be sterile if *hc163* did not suppress *spe-8*. Similar crosses were performed to test suppression of *fer-1(hc13*ts).

Genetic mapping of *hc163*: We used *trans*-heterozygote linkage analysis with respect to *dpy-1(e1)* to assign *hc163* to chromosome III. *cis*-heterozygote recombination mapping experiments with *hc163 dpy-1(e1)* and *hc163 dpy-18(e364)* double mutants were performed to map *hc163* more accurately. Genetic mapping data are available on the world wide web at WormBase (http://www.wormbase.org).

Complementation crosses between *hc163* and chromosome III deficiencies: We tested chromosome III deficiencies *tDf2*, *tDf7*, *ctDf3*, and *ctDf2* for their ability to complement *hc163*. *hc163; spe-27(it132) unc-22(e66)* hermaphrodites were crossed to *tDf2/qC1 dpy-19(e1259) glp-1(q339); spe-27(it132)* males. Individual F_1 hermaphrodite progeny were scored for fertility at 25°. If *hc163* complements the deficiency, then all F_1 hermaphrodites should be sterile; if *hc163* fails to complement the deficiency, then about one-half of the F_1 hermaphrodites should be fertile. As a negative control, similar crosses were assayed using *spe-27(it132) unc-22(e66)* worms as the hermaphrodite parent. Similar complementation crosses and controls were done with the other three deficiencies.

Complementation tests between *hc163* and *spe-6(hc49)*: We performed two different tests to determine if *hc163* and *spe-6(hc49)* complement. First, we tested the ability of *hc163* to complement the sterile phenotype of *spe-6(hc49)*. Next, we tested whether *spe-6(hc49)* could complement the ability of *hc163* to suppress the temperature-sensitive self-sterile phenotype imposed by *spe-27(it132)*. For the first test, *spe-6(hc49) vab-7(e1562)* hermaphrodites were crossed to *hc163 dpy-18 (e364); him-5(e1490)* males. For the second test, *spe-6(hc49) vab-7(e1562); spe-27(it132)* hermaphrodites were mated to *hc163 dpy-18(e364); spe-27(it132); him-5(e1490)* males. F_1 hermaphrodites were picked to individual plates and assayed for self-fertility at 25°. For both tests, individual F_1 hermaphrodites were assayed for self-fertility at 25°.

Physical mapping of *ctDf3* and *tDf7* breakpoints: The ge-

nome sequence around the *spe-6* locus [yeast artificial chromosome (YAC) clone Y66D12, GenBank accession no. AL161712] was determined and generously provided by John Sulston and Alan Coulson (Sanger Center, Cambridge, UK). To locate the left breakpoint of *ctDf3* and the right breakpoint of *tDf7* on the *C. elegans* physical map, we designed PCR primers targeting sequences in the region and assayed their ability to amplify targets from individual arrested embryos homozygous for either deficiency. *ctDf3* or *tDf7* mutant embryos were treated essentially as described by Williams (1995), except that PCR reactions were performed with AmpliTaq Gold DNA polymerase (PE Biosystems), using the manufacturer's recommended cycling parameters. For every PCR reaction, we included, in addition to the experimental target primers, negative control primers targeting a region known to be deleted in the deficiency and positive control primers targeting a region known not to be deleted in the deficiency. Only reactions displaying the positive control PCR product and lacking the negative control fragment were scored. We typically tested 12 individual embryos for each target primer set.

Sequencing *spe-6* mutants and cDNAs: To sequence *spe-6* wild-type and mutant alleles, fragments of the *spe-6* genomic region of homozygotes were first amplified by single-worm PCR using similar conditions as used for mapping deficiency breakpoints. Four PCR reactions were run for each template, and the products were pooled and purified by filtration on a Microcon PCR purification filter (Millipore, Bedford, MA). cDNA clones for sequencing were amplified from a *C. elegans* spermatogenesis-enriched library constructed and generously provided by H. Smith (unpublished results). Automated DNA sequencing was performed by the Laboratory of Molecular Systematics and Evolution (Arizona Research Labs, University of Arizona). Data were analyzed using the Wisconsin Package Version 10.0 for UNIX (Genetics Computer Group, Madison, WI) and FAKtory (Miller and Myers 1999).

Microinjection transformation rescue: Using TurboPfu polymerase (Stratagene, La Jolla, CA), we amplified a 3.8-kb fragment from wild-type worms containing the entire putative *spe-6* gene (Y66D12A.20), including 180 bases 3′ of the stop codon, and all of the upstream sequences, including the 5′ portion of the immediately upstream gene (Y66D12A.21). For microinjection rescue, we injected a mixture containing the PCR fragment (2 ng/μl), linearized plasmid *pRF4* (2 ng/μl; Kramer *et al.* 1990; Mello and Fire 1995), and *Pvu*II-digested *C. briggsae* genomic DNA (100 ng/μl; Kelly *et al.* 1997) into young adult *spe-6(hc49) vab-7(e1562); eDp6* hermaphrodites. Non-Vab, rolling F_1 progeny (which retain the complementing free duplication) were saved and allowed to produce a subsequent generation (F_2). F_2 Vab (*i.e.*, lacking *eDp6*) rollers were assayed for self-fertility. For negative controls we injected DNA mixes lacking the *spe-6* PCR fragment, as well as neighboring cosmids and PCR fragments encoding several other genes in the vicinity.

Progeny counts: To determine brood sizes, virgin L4 hermaphrodites were incubated on individual culture plates at 20° (unless otherwise noted) and transferred to fresh plates daily until they stopped laying eggs. To count dead and live progeny, plates were incubated for at least 24 hr after the parents were removed to allow all viable eggs to hatch. Live progeny and dead embryos were counted daily as they were aspirated from the plate.

Light microscopy: Differential interference contrast (DIC) images of live worms or dissected testes in SM1 buffer (Machaca *et al.* 1996) were observed on a Leica DM-RXA microscope and captured digitally with a Hamamatsu C4742-98 CCD camera controlled with MetaMorph imaging software (Universal Imaging, West Chester, PA).

Electron microscopy: Four-day-old virgin *spe-6(hc163); him-5(e1490)* or *him-5(e1490)* males were prepared as described by Varkey *et al.* (1993). Thin sections were collected on carbon-stabilized, pilloform-coated grids, stained in uranyl acetate and lead citrate, and examined at 80 kV on a JEOL H-500 electron microscope.

RESULTS

Isolation and characterization of suppressors of a spermiogenesis initiation mutant: To search for additional genes in the spermiogenesis initiation pathway and to reveal potential interactions among the four known genes, we selected for ethyl methanesulfonate-induced fertile suppressors of *spe-27(it132)*, a temperature-sensitive missense allele. At 25°, homozygous *it132* virgin hermaphrodites are self-sterile, but mated hermaphrodites are cross- and self-fertile (Minniti *et al.* 1996). At 15°, each *it132* virgin hermaphrodite produces ~30 progeny, enabling us to grow a large population of homozygous mutants for secondary mutagenesis.

We isolated 32 recessive suppressors of *it132* whose self-brood sizes (in a homozygous *it132* genetic background) range from 5 to 82 progeny at 25°. We chose 14 suppressor strains with the highest self-fertility (14–82 progeny) for initial characterization. None of the suppressor mutations are alleles of *spe-27*. All 5 of the most fertile suppressors (*hc163*, *hc164*, *hc165*, *hc166*, and *hc167*) failed to complement each other, and *hc163* failed to complement the remaining 9 recessive suppressor strains. Further genetic and phenotypic analysis was restricted to allele *hc163*, which suppressed *spe-27(it132)* to yield 82 ± 21 progeny at 25°, where *spe-27(it132)* produced no progeny and wild type produced 188 ± 47 progeny.

***hc163* mutants suppress mutations in multiple genes required for spermiogenesis initiation:** To determine whether the Spe-27-suppression phenotype results from an allele-specific interaction with *spe-27(it132)*, we tested whether *hc163* could suppress two probable null alleles of *spe-27*, *it110*, and *hc161* (Minniti *et al.* 1996). The *hc163* mutation restored self-fertility to both *it110* and *hc161* hermaphrodites (Table 1), suggesting that *hc163* obviates the requirement for the SPE-27 gene product altogether. We next asked if *hc163* could suppress mutations in three other genes required for spermiogenesis initiation, *spe-8*, *spe-12*, and *spe-29* (Table 1). These genes appear to act in concert in spermiogenesis initiation (Nance *et al.* 1999, 2000). We found that *hc163* restored fertility to mutants in all three genes, indicating that *hc163* can bypass the role of this group of gene products in initiating spermiogenesis. In contrast, *hc163* failed to suppress mutations in *fer-1*, a gene required for a later step in spermiogenesis (Achanzar and Ward 1997; Table 1). Thus, *hc163* appears to bypass specifically the initial steps of the spermiogenesis signaling pathway.

***hc163* is an allele of *spe-6*, a gene required for early events in sperm development:** We mapped *hc163* and

TABLE 1

Suppression of spermiogenesis mutants by *hc163*

Parental genotype	Fertile F_1s
hc163 / + *III*; *spe-27(it132)* / *spe-27(it110)* *unc-22(e66)* + / + *dpy-20(e1282)* *IV*[a]	7/37 (19%) of Dpy non-Uncs
hc163 / + *III*; *spe-27(it132)* / *spe-27(hc161)* *unc-22(e66)* / + *IV*[a]	8/41 (20%) of non-Uncs
hc163 / + *III*; *spe-29(it127)* / + *dpy-20(e1282)* + / + *spe-27(it132)* *unc-22(e66)* *IV*[b]	17/71 (24%) of Dpys
hc163 / + *III*; *spe-12(hc76)* / + *dpy-5(e61)* / + *IV*[a]	34/110 (31%) of Dpys
spe-8(hc79) / + *I*; *hc163* / + *dpy-18(e364)* / + *III*[a]	76/76 (100%) of Dpys
fer-1(hc13) *unc-29(e1072)* / + + *I*; *hc163* *dpy-18(e364)* / + + *III*[b]	0/38 (0%) of Dpy Uncs

The left column shows the parental genotype for each cross. The right column shows the fraction of F_1 hermaphrodite progeny of the relevant morphological phenotype that were fertile at 25°. Morphological markers in the F_1 progeny indicate homozygosity of the linked spermiogenesis defect mutation being tested for the crosses involving *spe-27*, *spe-29*, and *spe-12*, and they indicate the homozygosity of *hc163* for the cross involving *spe-8*. For the cross involving *fer-1*, Dpy Uncs should be homozygous for both the *fer-1* mutation and *hc163*. For the first four crosses, ~25% of the scored progeny should be fertile if *hc163* suppresses the *spe* mutation; none of the scored progeny (except for rare recombinants) should be fertile if *hc163* does not suppress the *spe* mutation. For the last two crosses, the expected fraction of scored progeny that are fertile is 100% if *hc163* suppresses and 0% if it does not suppress (barring rare recombinants). Genetic distances (20°) between markers are *spe-27* and *unc-22*, 2.9 cM; *spe-27* and *dpy-20*, 2.6 cM; *spe-12* and *dpy-5*, 2.6 cM; *hc163* and *dpy-18*, 1.1 cM; *fer-1* and *unc-29*, 0.28 cM.

[a] Hermaphrodites and males were crossed.

[b] Hermaphrodites were selfed.

the other 13 suppressor mutations to chromosome III, ~1 cM to the right of *dpy-18*. Complementation tests localized the mutation under deficiencies *tDf7* and *ctDf3* and between *tDf2* and *ctDf2* (Figure 1A). The combination of complementation and genetic mapping data suggested that all of these mutations are alleles of the same gene. We confirmed this by sequence analysis (described below) and identified four additional alleles of this gene in our collection of suppressors. Genetic analysis of the remaining nine suppressor strains, most of which have very low fertility, indicated that their mutations are not allelic to *hc163*. We will describe these mutants elsewhere.

The only reported mutations in the genetic interval containing *hc163* were in *spe-6*, a gene originally defined in our laboratory by four mutations—*hc49*, *hc92*, *hc143*, and *hc146*—which behave as loss-of-function or strong reduction-of-function alleles and affect an early stage of sperm development (Varkey *et al.* 1993). Spermatocytes from these mutants fail to assemble MSP into fibrous bodies. Instead, MSP is distributed throughout the spermatocyte cytoplasm. These mutant spermatocytes fail to complete meiosis, missegregate chromosomes and organelles, and fail to develop further into spermatids, resulting in a sterile (Spe) phenotype. Despite the differences between this phenotype and the spermiogenesis-defect suppression phenotype, we tested whether the suppressor mutants are alleles of *spe-6*. *spe-6 (hc49)* failed to complement the Spe-27-suppression phenotype of *hc163*, and *hc163* partially failed to complement the sterile phenotype of *spe-6(hc49)*, indicating that the suppressor mutants are indeed *spe-6* alleles.

Identifying the *spe-6* gene: *spe-6* is the only reported locus that genetically maps to a region of chromosome III deleted in deficiencies *tDf7* and *ctDf3*, which suggested that this region might be physically small (Figure 1A). To locate this region on the physical map we performed PCR assays on individual dead embryos homozygous for *tDf7* or *ctDf3* using primer sets designed from the published DNA sequence in this region of the genome. We narrowed the *tDf7/ctDf3* overlap to within a 12-kb region represented in YAC clone Y66D12 (GenBank accession no. AL161712; Figure 1B).

We surveyed the genes in this region by performing a BLASTN search against the *C. elegans* expressed sequence tag (EST) nucleotide database (Altschul *et al.* 1990, 1997). Three closely spaced genes were indicated by near-perfect matches to *C. elegans* ESTs. The most

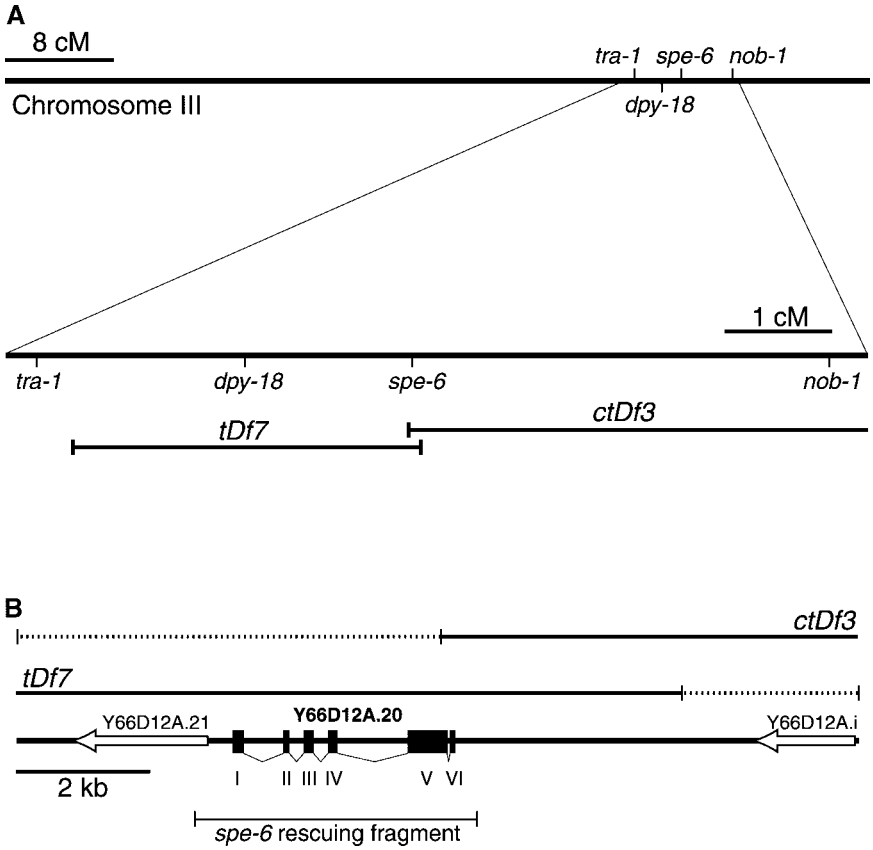

FIGURE 1.—Location of the *spe-6* gene. (A) Genetic map of chromosome III showing *spe-6* and nearby genetic markers. The enlarged map shows the genetic positions of chromosome deficiencies *tDf7* and *ctDf3*. The bars represent corresponding regions of chromosome III that are deleted in each deficiency. *spe-6* is deleted by *tDf7* near its right breakpoint; *ctDf3* deletes *spe-6* near its left breakpoint. (B) Physical map of the *spe-6* locus. *tDf7* and *ctDf3* are shown as lines above a 12-kb region of YAC Y66D12. The solid lines bounded by vertical bars represent regions of the genome confirmed to be deleted by either deficiency. Dotted lines represent the limits to which the left breakpoint of *ctDf3* or right breakpoint of *tDf7* were mapped. The *spe-6* gene (Y66D12A.20) is shown as black rectangles, representing exons. The two white arrows are the closest flanking genes to *spe-6* as indicated by BLASTN alignment of the region to the *C. elegans* EST database (the left gene, Y66D12A.21, encodes yk633c9, GenBank accession no. AV194753; the right gene, Y66D12A.i, encodes yk133c4, GenBank accession no. D68592). Two additional small genes, Y66D12A.18 and Y66D12A.19, are predicted by the *C. elegans* Sequence Consortium to lie between *spe-6* and Y66D12A.i, but are not confirmed by matches to cDNAs or sequence similarity to other known genes. The boundaries of the ~4-kb PCR fragment, containing the entire *spe-6* gene and a small portion of the upstream coding sequence of the neighboring gene, which rescued the sterile phenotype of *spe-6(hc49)* mutants, is shown below the *spe-6* gene.

attractive *spe-6* candidate, Y66D12A.20, matched not only cDNAs from a male/hermaphrodite mixed stage library, but cDNAs previously characterized in our laboratory from a collection of spermatogenesis-specific clones (ca01c03, GenBank accession nos. AW057333 and AW057136; H. SMITH, unpublished results). We sequenced this gene from several *spe-6(hc163)* mutant individuals and found a single missense mutation in an exonic region. We subsequently identified mutations in this gene in the other *spe-6* alleles (described in detail below). As further confirmation that this gene is *spe-6*, a PCR-amplified fragment containing only this gene (Figure 1) efficiently rescued the sterile phenotype of *spe-6(hc49)* mutants, yielding 210 ± 54 ($N = 17$) progeny per transformant at 20°.

***spe-6* encodes a casein kinase 1:** BLASTP and TBLASTN searches of the public sequence databases revealed that the predicted SPE-6 protein (Wormpep ID WP:CE28799) is a member of the CK1 family of protein-serine/threonine kinases (Figures 2 and 4). SPE-6 shares ~30% identity and almost 50% similarity to yeast, mammalian, and plant CK1 proteins over their catalytic domains. *C. elegans* has a large CK1 subfamily, containing ~90 members (PLOWMAN *et al.* 1999). SPE-6 shows slightly higher sequence similarity to these than to those of other phyla. As with other protein-serine/threonine kinases, SPE-6 has a highly conserved catalytic domain of ~286 amino acids (HANKS *et al.* 1988; GROSS and ANDERSON 1998). It has a short N terminus and an ~70-amino-acid C terminus whose sequences share no significant similarity with other proteins. On the basis of the longest 5′ cDNA end detected, we tentatively assign the first in-frame methionine codon in exon 1 as the start codon, although the *C. elegans* Sequencing Consortium predicts an additional 9 amino acids at the N terminus of Y66D12A.20 (Figure 3).

Identification of *spe-6* mutations: We identified mutations in all four of the *spe-6* sterile alleles and 18 suppressor alleles (Figures 2–4). The canonical sterile allele, *hc49*, contains a premature stop codon predicted to result in a protein truncated at a position in the C-terminal domain. *hc146* is identical to *hc49* and may be a reisolate of the original mutation. Two independently isolated sterile alleles, *hc92* and *hc143*, are both T185I substitutions. This is also likely to be a null mutation because this residue is universally conserved as a threonine or serine in all CK1 proteins (and most other protein kinases) examined, and it may participate in a hydrogen-bonding network that stabilizes the catalytic core of the enzyme (KARLSSON *et al.* 1993; ZHANG *et al.* 1994). In addition, the *hrr25-2* mutant allele of a *Saccharomyces cerevisiae* casein kinase 1, which has drasti-

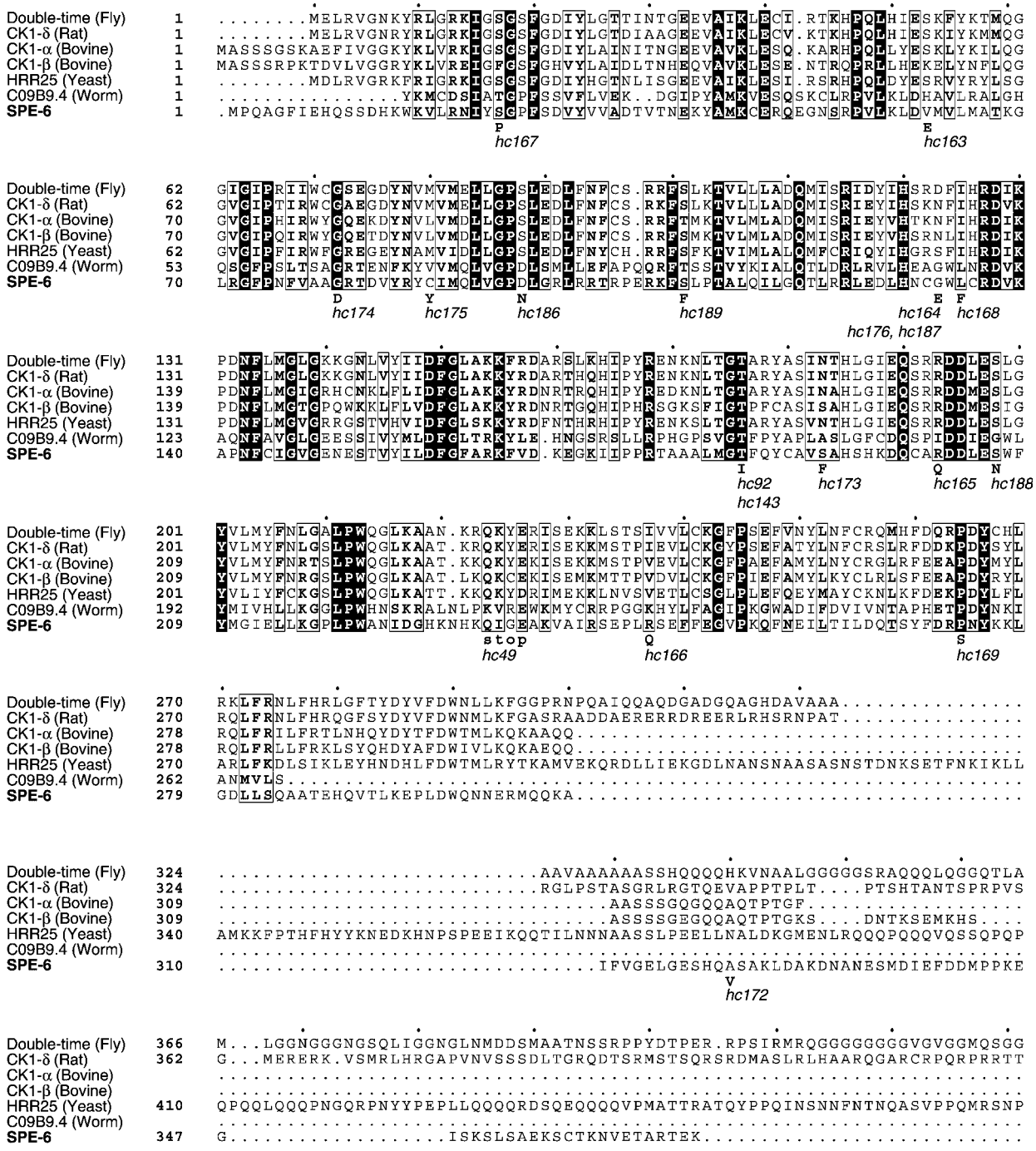

FIGURE 2.—Multiple sequence alignment of SPE-6 with several other casein kinase 1 proteins. The alignment was performed using Clustal X (JEANMOUGIN *et al.* 1998) and formatted with ESPript (http://prodes.toulouse.inra.fr/ESPript/). Amino acid postions are numbered at left. Universally conserved residues are on a black background; strongly conserved positions are boxed. Gaps introduced in sequences to facilitate alignment and regions beyond the C and N termini are marked on the sequence line with a period. Below the sequence alignments amino acid changes represented by various SPE-6 mutant alleles are marked. Sequences used for the alignments are *Drosophila melanogaster* double-time (discs overgrown protein), PID g6014927 (KLOSS *et al.* 1998); rat casein kinase I, δ isoform, PID g547766 (GRAVES *et al.* 1993); bovine casein kinase I, α isoform, PID g547763 (ROWLES *et al.* 1991); bovine casein kinase I, β isoform, PID g547764 (ROWLES *et al.* 1991); yeast HRR25 protein, PID g171706 (HOEKSTRA *et al.* 1991); SPE-6; and *C. elegans* hypothetical protein C09B9.4, PID g7495729 (H. Bradshaw, direct GenBank submission).

cally reduced kinase activity, has an identical substitution of the corresponding residue (T176I; MURAKAMI *et al.* 1999).

As shown in Figure 4, SPE-6 mutations that lead to the spermiogenesis-defect suppression phenotype are distributed mainly throughout the catalytic domain of

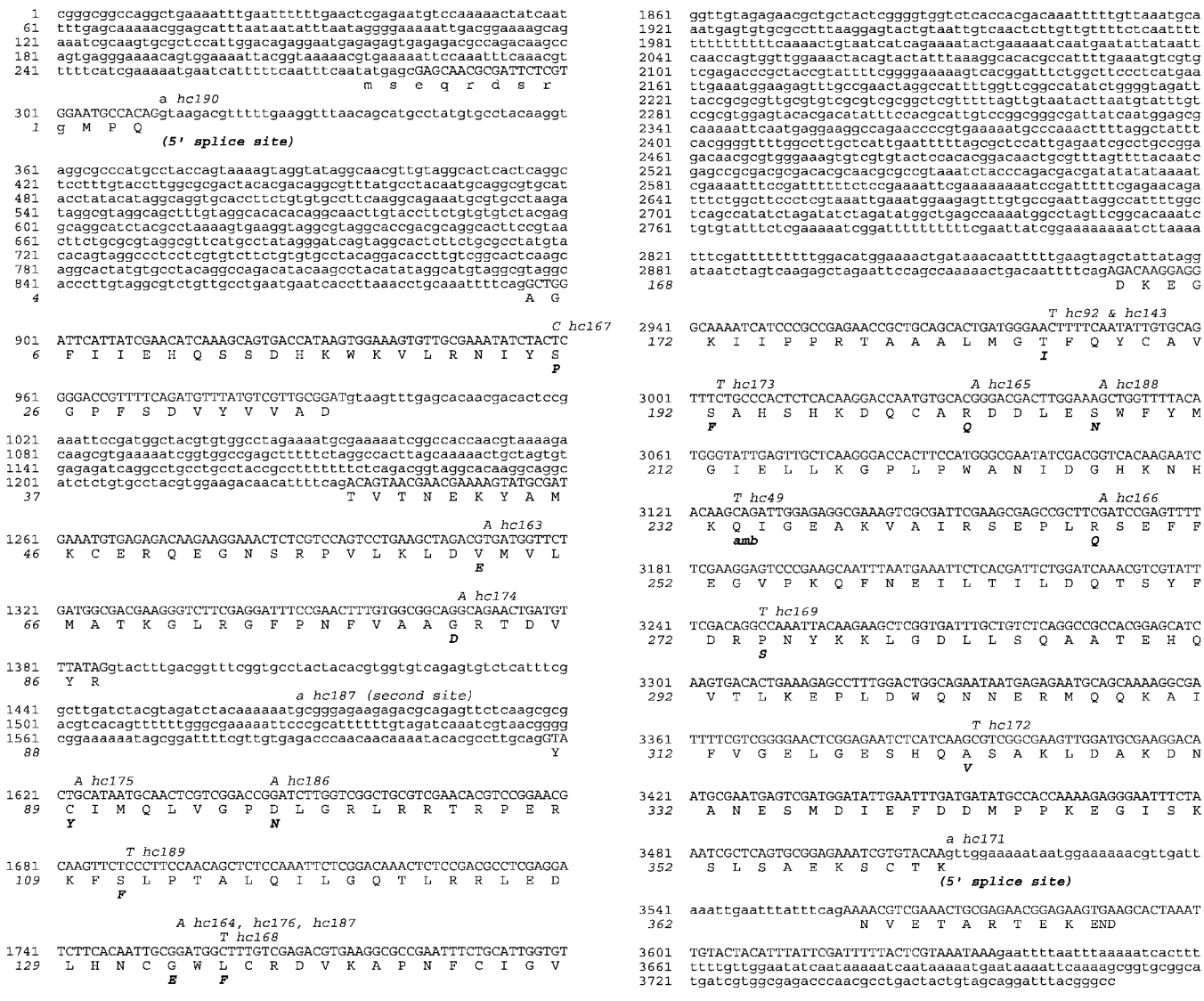

FIGURE 3.—Sequence of the *spe-6* gene and predicted amino acid sequence of the wild-type and mutant alleles of the SPE-6 protein. The nucleotide changes of mutant alleles are shown in italic above the DNA sequence; their predicted protein alterations are shown below the sequence in bold italic. The predicted protein-coding sequence is shown in uppercase; noncoding sequence is in lowercase. A nine-residue extension of the polypeptide N terminus predicted by the *C. elegans* Sequencing Consortium, but not confirmed by the presence of corresponding cDNA clones, is shown in lowercase. Nucleotide and amino acid positions (italic) are numbered at left. Nucleotide numbering starts from the first base upstream of the 5′ end of the longest EST (yk633c9, GenBank accession no. AV194753) encoded by the divergently transcribed upstream neighboring gene (Y66D12A.21) and ends at the 3′-most base in the PCR fragment that rescues *spe-6(hc49)* mutants. This corresponds to nucleotide positions 17844–21613 in the sequence for Y66D12A, GenBank accession no. AL161712. "*amb*" denotes an amber nonsense codon in allele *hc49*.

the protein. Some of the suppressor mutations are predicted to lie in regions of the protein recognized as important for its kinase activity, such as the ATP-binding region [*e.g.*, *hc167*(S24P)] and the catalytic cleft [*e.g.*, *hc164*, *hc176*, *hc187* (all G133E), and *hc168* (L135F)]. However, no suppressor mutations are in positions known to be essential for activity in related protein kinases. Several mutations are in regions of the protein where functions are not well characterized. Of the 18 suppressor alleles, 16 have single amino acid substitutions. *hc190* has a mutation in the conserved 5′ intronic G of the first intron, within the N terminus, and probably results in a misspliced message. *hc171* has a disrupted 5′ splice donor site in the final intron; the effects of this on its transcript and protein products are not known. Beside *hc171*, the only other mutation in the C terminus is *hc172* (A322V).

Spe-6(hc163) phenotypes: The suppression phenotype of *spe-6* suppressor alleles indicates that, in mutant hermaphrodites, spermatids initiate spermiogenesis without requiring the activation signal transduced by the *spe-8*, *-12*, *-27*, *-29* signaling pathway. Using transmission

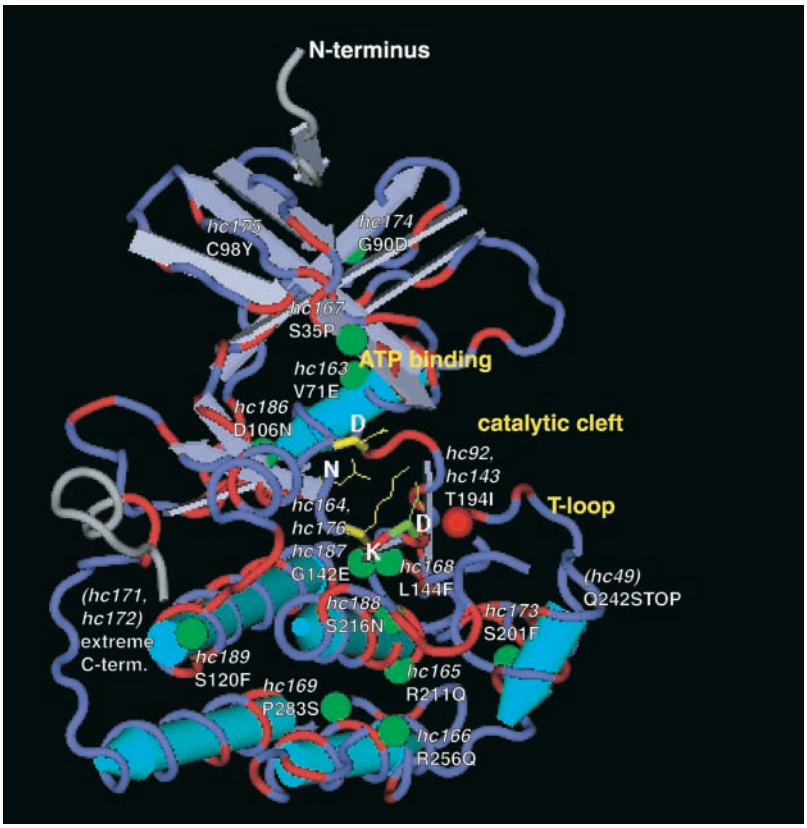

FIGURE 4.—A model structure for SPE-6. An alignment of the predicted SPE-6 polypeptide sequence mapped onto the crystal structure of the mammalian casein kinase 1 δ catalytic region (residues 1–317 PDB Id 1CKI) using the computer program Cn3D (http://www.ncbi.nlm.nih.gov/Structure/CN3D/cn3d.shtml). Red segments of the polypeptide backbone show amino acid identities; nonidentical residues are in blue. β-sheets are shown as light blue arrows and α-helices are teal pointed cylinders. SPE-6 mutations are shown as red (sterile alleles) or green (suppressor alleles) spheres. Side chains are shown for four universally conserved residues that form the catalytic center in virtually all serine-threonine protein kinases (yellow or green sticks). The T194I mutation in sterile alleles *hc92* and *hc143* alters a threonine that normally H-bonds to the catalytic aspartic acid. This figure is a likely approximation to the three-dimensional structure based on the strong conservation between SPE-6 and the mammalian protein. Although it may not be correct in detail, it is useful for visualizing the location of mutations in SPE-6 in the conserved regions of the protein.

electron microscopy, we found that spermatids from *hc163* mutant virgin males also activate precociously to form spermatozoa (Figure 5A). However, it is clear that only a small fraction of the spermatids develop into mature spermatozoa in males. Interspersed among the spermatozoa are what appear to be the cytoplasmic contents of degraded cells. The degraded cells were presumably spermatids because the zone of degradation is restricted to the proximal end of the testis, where spermatids normally accumulate. Additionally, nuclei in the degradation zone have the highly compact morphology of spermatid nuclei rather than the more typical structure of spermatocyte nuclei (Figure 5A). This cellular lysis appears similar to the necrosis-like cell death seen in several *C. elegans* mutants that affect ion transport in sensory neurons (DRISCOLL 1996; HALL *et al.* 1997; BERGER *et al.* 1998; CHUNG *et al.* 2000).

In marked contrast to the sterile *spe-6* mutants, whose membranous organelles lack fibrous bodies altogether, fully developed spermatocytes from *hc163* mutants have normal looking FB-MO complexes. In early stage spermatocytes, however, the developing FB-MO complexes contain FBs with ragged edges, separated from the membrane of the MO (Figure 5, F and G).

hc163 appears to affect fertility more severely in males than in hermaphrodites. While mutant males copulate normally, their crosses are rarely successful, and those that are successful result in very few cross-progeny (data not shown). This is consistent with the severe ultrastructural defects and reduced number of spermatozoa we observed in mutant male testes. Hermaphrodites show minimal signs of sperm degradation by light microscopy (data not shown).

On the basis of their recessive behavior and their intermediate effects on fertility and testis ultrastructure, the *spe-6* suppressors appear to be reduction-of-function alleles. We asked whether *hc163* could be a gain-of-function allele, even though such mutations are usually dominant. If *hc163* were a gain-of-function allele, then two doses of the mutation should cause a more severe phenotype (*i.e.*, lower fertility) than a single dose, but this is not the case (Table 2). The recessive nature and partial sterile phenotypes of the other *spe-6* suppressor mutants, together with the observation that their lesions are widely distributed throughout the predicted protein, support the notion that these suppressors are also reduction-of-function alleles.

DISCUSSION

We show here that certain alleles of *spe-6*, a gene known from previous work to be required early in sperm development, can suppress mutations in all four of the known genes required for spermiogenesis initiation, one of the final events in sperm development. The proteins encoded by the three cloned spermiogenesis initiation genes, *spe-12*, *spe-27*, and *spe-29*, show no significant similarity to any other proteins in the sequence data-

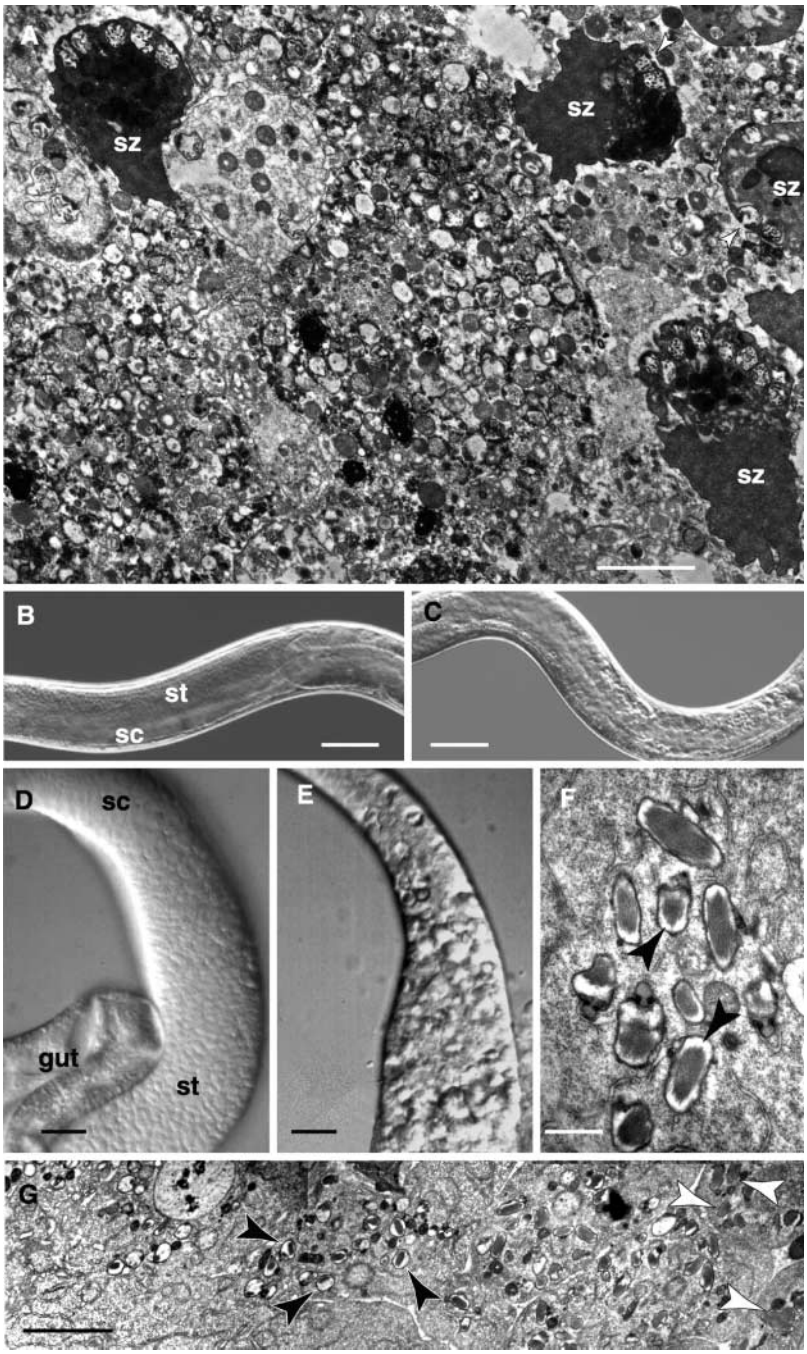

FIGURE 5.—*spe-6(hc163)* microscopic phenotypes. (A) Transmission electron micrograph (TEM) of a portion of the proximal testis of a *spe-6(hc163); him-5(e1490)* young adult virgin male. Note the presence of mature spermatozoa (sz) containing extended pseudopods and fused MOs (arrowheads). Also note the abundant cellular debris surrounding the spermatozoa (bar, 2 μm). (B) DIC micrograph of a wild-type (N2) young adult virgin male. Note the smooth regular appearance of packed spermatids (st) and spermatocytes (sc; bar, 50 μm). (C) DIC micrograph of *spe-6(hc163)* young adult virgin male. Note rough uneven appearance of testis (bar, 50 μm). (D and E) DIC micrograph of testes from virgin wild-type (D) and *spe-6(hc163)* (E) males. Note smooth packed spermatids and spermatocytes in wild type and disorganized appearance in the mutant (bars, ~10 μm). (F) TEM of FB-MOs from early *spe-6(hc163); him-5(e1490)* male spermatocytes, showing that FBs do not completely fill the MOs (black arrowheads), as they do in wild type (not shown; bar, 1 μm). (G) TEM of distal portion of the testis of a *spe-6(hc163); him-5(e1490)* young adult virgin male showing developing spermatocytes. The most distal region (youngest spermatocytes) is at left. Note that in the youngest spermatocytes, fibrous bodies are separated from the membranous organelle membranes (black arrowheads). FB-MOs in more mature spermatocytes (white arrowheads) appear normal (bar, 5 μm).

bases, and the nature of their activities is unknown. SPE-12 resides in the spermatid plasma membrane, and genetic interactions between *spe-12*, *-27*, and *-29* suggest that their products may act together in a complex (NANCE *et al.* 1999, 2000). The suppression of all four genes by *spe-6* mutations provides additional evidence that they act in a common pathway and suggests that SPE-6 is a downstream target of that pathway. The sequence similarity of SPE-6 to the casein kinase 1 family and the observation that several SPE-6 mutations lie in the putative kinase catalytic region and in other highly conserved residues of protein-serine/threonine kinases strongly suggest that SPE-6 is a protein kinase and that its kinase activity is essential to its function both early and late in sperm development.

The role of *spe-6* in spermiogenesis initiation: Because an apparent reduction of SPE-6 activity suppresses spermiogenesis-defective mutations, we propose that the normal function of the SPE-6 protein kinase in spermatids is to restrain the spermiogenesis machinery, preventing it from engaging until the SPE-8, -12, -27, and -29 gene products have relayed the signal to commence spermiogenesis (Figure 6A). In this model, SPE-6 maintains phosphorylation of its target protein substrate(s), which in turn serves as a brake on spermiogenesis. When stimulated by an extracellular signal, the SPE-8, SPE-12,

TABLE 2

Self-fertility of hermaphrodites with differing doses of *spe-6(+)* or *spe-6(hc163)*

Genotype	Mean progeny[a] ±SEM (*N*)
spe-6(hc49)/spe-6(h49)	0 ± 0 (10)
spe-6(hc163)/spe-6(hc163)	262 ± 9.2 (14)[c]
spe-6(hc163)/ctDf3[b]	242 ± 12.4 (12)[c]
spe-6(hc163)/+	358 ± 7.7 (15)
Wild type (N2)	306 ± 13.5 (10)

[a] Total number of live and dead progeny. The genotype caused significant differences in the total numbers of progeny produced (ANOVA: $F_{(3,47)} = 22.064$, $P = 0.000$). Except where noted below, each mean progeny size differs significantly from the others ($P \leq 0.05$, Tukey post-hoc test). Data for *spe-6(hc49)* were not included in the statistical analysis because they lack variance.

[b] *ctDf3* is a deficiency chromosome that deletes the *spe-6* locus. Its complete genotype is *ctDf3* [*dpy-18(e364) unc-25 (e156)*]III.

[c] These mean progeny sizes are not significantly different from each other.

SPE-27, and SPE-29 gene products antagonize the SPE-6 kinase activity, releasing the brake so that spermiogenesis can proceed, forming the crawling spermatozoon (Figure 6B).

Casein kinase 1 proteins are ubiquitous and promiscuous regulatory proteins, engaged in a wide range of cellular processes (Gross and Anderson 1998). While CK1 proteins share extensive sequence similarity with each other over their catalytic domains, many have divergent C-terminal tails. These are often phosphorylation substrates themselves and are probably important for regulating activity and substrate specificity (Cegielska *et al.* 1998; Rivers *et al.* 1998; Gietzen and Virshup 1999). Since SPE-6 contains a long unique C terminus, rich in serines and threonines, regulation by the *spe-8, -12, -27, -29* pathway could inhibit SPE-6 by altering phosphorylation of sites in its C terminus. Preliminary experiments indicate that SPE-6 indeed exists in spermatids in several differently charged isoforms, possibly representing alternate phosphorylation states (M. Galligan and P. Muhlrad, unpublished results). Once SPE-6 kinase activity is inhibited, a phosphatase activity would be required to dephosphorylate the targets of SPE-6. Such phosphatases could be among the non-*spe-6* suppressors from our screen that are yet to be characterized.

Because spermatids lack translational machinery, spermiogenesis must be controlled by post-translational regulation; therefore it is not surprising that nematode sperm employ protein phosphorylation. *spe-6* is the first protein kinase gene demonstrated to regulate sperm development in *C. elegans*, but a protein-tyrosine kinase activity is key to sperm motility in the related nematode, *Ascaris suum* (Italiano *et al.* 1996, 1999). DNA microarray analysis of *C. elegans* germline gene expression indicates that, among spermatogenesis-enriched genes, the number of protein kinase genes is three times the random expectation, and the number of protein phosphatase genes is almost nine times the random expectation, suggesting that protein phosphorylation may indeed be a prominent mechanism for regulating spermatogenesis (Reinke *et al.* 2000).

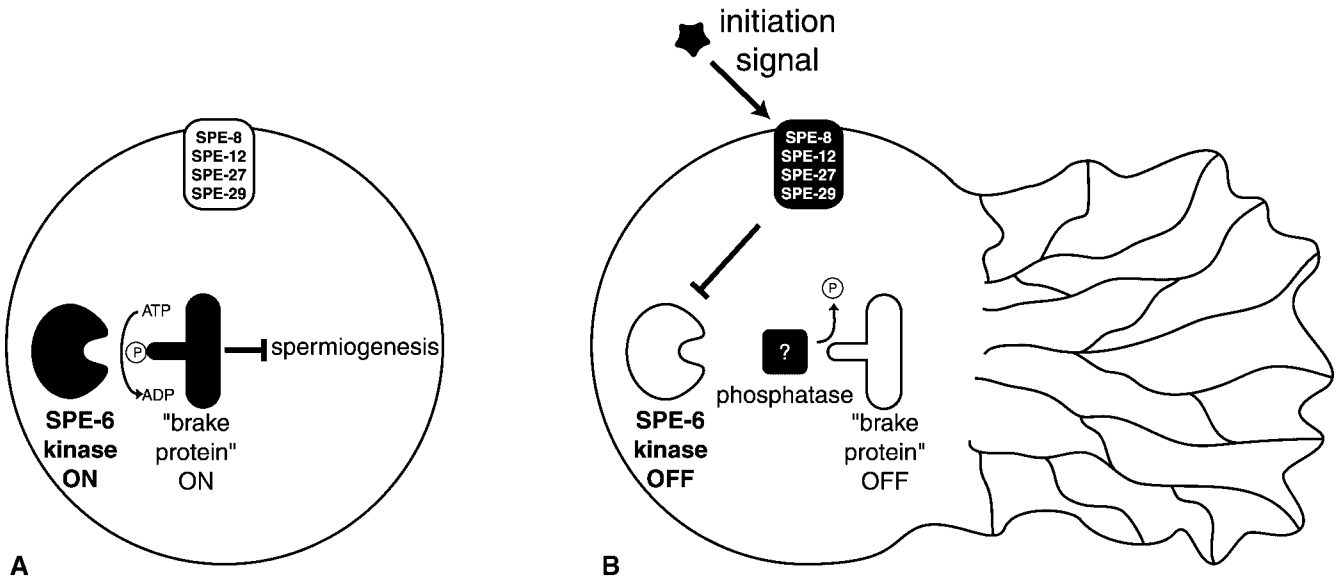

Figure 6.—A model for the role of SPE-6 in spermiogenesis initiation signaling. (A) In a spermatid that has not been exposed to the spermiogenesis initiation signal, the active SPE-6 protein kinase phosphorylates, and thereby activates, a spermiogenesis "brake protein." (B) Upon exposure of the spermatid to the initiation signal, the SPE-8, -12, -27, and -29 proteins inhibit SPE-6. A hypothetical phosphatase activity can then irreversibly dephosphorylate the spermiogenesis brake protein, rendering it inactive and ensuring that spermiogenesis proceeds completely.

The role of *spe-6* in early sperm development: We were surprised to discover that the suppressor mutations are alleles of *spe-6*, a gene our laboratory had previously found to be involved in spermatocyte development (Varkey *et al.* 1993). The sterile *spe-6* mutants appear to have loss-of-function or strong reduction-of-function alleles on the basis of their genetic behavior (Varkey *et al.* 1993) and their protein lesions: a polypeptide truncation and an alteration at a nearly universally conserved amino acid. These strong alleles result in spermatocytes that fail to assemble MSP into fibrous bodies and arrest development prior to forming spermatids. Thus, in contrast to its inhibitory role in spermiogenesis, SPE-6 activity is necessary for fibrous body formation and spermatocyte development. Because sterile *spe-6* mutants make no spermatids, we could not determine the effect of these alleles on spermiogenesis initiation. However, we did examine spermatocyte development in the suppressor mutants. The ultrastructural examination of *spe-6(hc163)* males suggests that *spe-6* suppressor alleles may affect fibrous body formation similarly as in sterile alleles, although less severely and only transiently. Microscopic examination and the low fertility of *hc163* males suggests that, like the null alleles, suppressor alleles cause reduced numbers of functional spermatids.

Relating the functions of SPE-6: How might SPE-6 perform apparently different functions in distinct stages of spermatogenesis? The need for SPE-6 for fibrous body formation in spermatocytes and its inhibitory role in spermiogenesis may reflect different phosphorylation targets in these two cells. Alternatively, SPE-6 may phosphorylate the same proteins in spermatocytes and spermatids, but these targets could lead to different effects based on their distinct cellular contexts. We cannot eliminate a third possibility—that the effect of *spe-6* mutations on spermiogenesis may be only an indirect consequence of its earlier influence on spermatocytes. Defective spermatocytes may simply produce spermatids that are incapable of repressing spermiogenesis. However, the sheer number of *spe-6* alleles that produce the suppression phenotype and the minimal ultrastructural defects observed in *hc163* mutant spermatocytes argue against this possibility.

How is fibrous body formation in spermatocytes related to spermiogenesis initiation in spermatids? One common feature of these two processes is that each involves MSP polymerization. SPE-6 may regulate the state of MSP polymerization, although not by directly phosphorylating it, since MSP is not detectably phosphorylated *in vivo* (Burke and Ward 1983). Evidence from both *C. elegans* and Ascaris suggests that MSP polymerization is controlled by intracellular pH (Ward *et al.* 1983; Roberts and King 1991; King *et al.* 1994; Italiano *et al.* 1999). SPE-6 may influence MSP polymerization in both spermatocytes and spermatids by regulating pH.

Whatever the roles of SPE-6 in spermatocyte development and in spermiogenesis initiation, our analysis of suppressor allele *hc163* illustrates that a single mutation can compromise the two processes to dramatically different extents. *spe-6(hc163)* homozygous hermaphrodites have virtually identical (moderate) fertility as hemizygotes, suggesting that the mutation causes only a slight reduction of function in the SPE-6 protein relative to wild type. Indeed, *spe-6(hc163)* exhibits very little effect on spermatocyte development. Yet, this allele strongly influences spermiogenesis initiation. The large number and widespread distribution of *spe-6* suppressor mutations is consistent with the hypothesis that a small reduction in SPE-6 activity is sufficient to prevent SPE-6 from inhibiting spermiogenesis initiation.

This sensitivity of spermiogenesis initiation to small decreases in SPE-6 activity makes good biological sense. Sperm are the limiting gamete in *C. elegans,* so reproductive fitness depends directly on the number of functional sperm (Ward and Carrel 1979). Because spermatozoa rely on their pseudopods to adhere to the walls of the spermathecae and to crawl back to the spermathecae when they are pushed out by passing eggs, any spermatids remaining in the reproductive tract after ovulation begins risk being expelled as eggs are laid. Therefore, if SPE-6 is the control point preventing spermiogenesis initiation, it must be able to disengage quickly and completely in response to the spermiogenesis initiation signal in order to ensure that all spermatids mature to spermatozoa rapidly. Thus, the sensitivity of spermiogenesis to small decreases in activity would ensure maximal utilization of sperm and result in the maximum number of progeny.

We extend thanks to our colleagues, Jeremy Nance, for stimulating discussions throughout this project, Craig LaMunyon, for help with statistics, and Harold Smith, for providing cDNA libraries. We thank Theresa Stiernagle, Michel Labouesse, and Barbara Robertson for providing nematode strains, and Brian James for helping with complementation tests. We are especially indebted to Alan Coulson, Lucy Matthews, and John Sulston for filling the "*spe-6* chasm" of the *C. elegans* physical map. Finally, we thank C. LaMunyon, J. Nance, members of the Ward lab, a Genetics editor, and an anonymous reviewer for their insightful comments on the manuscript. Some nematode strains used in this study were provided by the *Caenorhabditis* Genetics Center, which is funded by the National Center for Research Resources. This work was supported by National Institutes of Health research grant GM25243 to S.W.

LITERATURE CITED

Achanzar, W. E., and S. Ward, 1997 A nematode gene required for sperm vesicle fusion. J. Cell Sci. **110:** 1073–1081.

Altschul, S. F., W. Gish, W. Miller, E. W. Myers and D. J. Lipman, 1990 Basic local alignment search tool. J. Mol. Biol. **215:** 403–410.

Altschul, S. F., T. L. Madden, A. A. Schaffer, J. Zhang, Z. Zhang *et al.*, 1997 Gapped BLAST and PSI-BLAST: a new generation of protein database search programs. Nucleic Acids Res. **25:** 3389–3402.

Anderson, P., 1995 Mutagenesis. Methods Cell Biol. **48:** 31–58.

Berger, A. J., A. C. Hart and J. M. Kaplan, 1998 G alphas-induced neurodegeneration in Caenorhabditis elegans. J. Neurosci. **18:** 2871–2880.

Brenner, S., 1974 The genetics of *Caenorhabditis elegans*. Genetics **77:** 71–94.

Burke, D. J., and S. Ward, 1983 Identification of a large multigene family encoding the major sperm protein of Caenorhabditis elegans. J. Mol. Biol. **171:** 1–29.

Cegielska, A., K. F. Gietzen, A. Rivers and D. M. Virshup, 1998 Autoinhibition of casein kinase I epsilon (CKI epsilon) is relieved by protein phosphatases and limited proteolysis. J. Biol. Chem. **273:** 1357–1364.

Chung, S., T. L. Gumienny, M. O. Hengartner and M. Driscoll, 2000 A common set of engulfment genes mediates removal of both apoptotic and necrotic cell corpses in C. elegans. Nat. Cell Biol. **2:** 931–937.

Driscoll, M., 1996 Cell death in C. elegans: molecular insights into mechanisms conserved between nematodes and mammals. Brain Pathol. **6:** 411–425.

Edgley, M. L., D. L. Baillie, D. L. Riddle and A. M. Rose, 1995 Genetic balancers. Methods Cell Biol. **48:** 147–184.

Gietzen, K. F., and D. M. Virshup, 1999 Identification of inhibitory autophosphorylation sites in casein kinase I epsilon. J. Biol. Chem. **274:** 32063–32070.

Graves, P. R., D. W. Haas, C. H. Hagedorn, A. A. DePaoli-Roach and P. J. Roach, 1993 Molecular cloning, expression, and characterization of a 49-kilodalton casein kinase I isoform from rat testis. J. Biol. Chem. **268:** 6394–6401.

Gross, S. D., and R. A. Anderson, 1998 Casein kinase I: spatial organization and positioning of a multifunctional protein kinase family. Cell. Signal. **10:** 699–711.

Hall, D. H., G. Gu, J. Garcia-Anoveros, L. Gong, M. Chalfie *et al.*, 1997 Neuropathology of degenerative cell death in Caenorhabditis elegans. J. Neurosci. **17:** 1033–1045.

Hanks, S. K., A. M. Quinn and T. Hunter, 1988 The protein kinase family: conserved features and deduced phylogeny of the catalytic domains. Science **241:** 42–52.

Hodgkin, J., 1995 Genetic nomenclature guide. Caenorhabditis elegans. Trends Genet. **11** (Suppl.): 24–25.

Hoekstra, M. F., R. M. Liskay, A. C. Ou, A. J. DeMaggio, D. G. Burbee *et al.*, 1991 HRR25, a putative protein kinase from budding yeast: association with repair of damaged DNA. Science **253:** 1031–1034.

Horvitz, H. R., S. Brenner, J. Hodgkin and R. K. Herman, 1979 A uniform genetic nomenclature for the nematode Caenorhabditis elegans. Mol. Gen. Genet. **175:** 129–133.

Italiano, J. E., Jr., T. M. Roberts, M. Stewart and C. A. Fontana, 1996 Reconstitution in vitro of the motile apparatus from the amoeboid sperm of Ascaris shows that filament assembly and bundling move membranes. Cell **84:** 105–114.

Italiano, J. E., Jr., M. Stewart and T. M. Roberts, 1999 Localized depolymerization of the major sperm protein cytoskeleton correlates with the forward movement of the cell body in the amoeboid movement of nematode sperm. J. Cell Biol. **146:** 1087–1096.

Italiano, J. E., Jr., M. Stewart and T. M. Roberts, 2001 How the assembly dynamics of the nematode major sperm protein generate amoeboid cell motility. Int. Rev. Cytol. **202:** 1–34.

Jeanmougin, F., J. D. Thompson, M. Gouy, D. G. Higgins and T. J. Gibson, 1998 Multiple sequence alignment with Clustal X. Trends Biochem. Sci. **23:** 403–405.

Karlsson, R., J. Zheng, N. Xuong, S. S. Taylor and J. M. Sowadski, 1993 Structure of the mammalian catalytic subunit of cAMP-dependent protein kinase and an inhibitor peptide displays an open conformation. Acta Crystallogr. Sect. D Biol. Crystallogr. **49:** 381–388.

Kelly, W. G., S. Xu, M. K. Montgomery and A. Fire, 1997 Distinct requirements for somatic and germline expression of a generally expressed *Caernorhabditis elegans* gene. Genetics **146:** 227–238.

Kimble, J., and S. Ward, 1988 Germ-line development and fertilization, pp. 191–213 in *The Nematode Caenorhabditis elegans*, edited by W. B. Wood. Cold Spring Harbor Laboratory Press, Plainview, NY.

King, K. L., J. Essig, T. M. Roberts and T. S. Moerland, 1994 Regulation of the Ascaris major sperm protein (MSP) cytoskeleton by intracellular pH. Cell Motil. Cytoskeleton **27:** 193–205.

Kloss, B., J. L. Price, L. Saez, J. Blau, A. Rothenfluh *et al.*, 1998 The Drosophila clock gene double-time encodes a protein closely related to human casein kinase Iepsilon. Cell **94:** 97–107.

Kramer, J. M., R. P. French, E. C. Park and J. J. Johnson, 1990 The Caenorhabditis elegans rol-6 gene, which interacts with the sqt-1 collagen gene to determine organismal morphology, encodes a collagen. Mol. Cell. Biol. **10:** 2081–2089.

Lewis, J. A., and J. T. Fleming, 1995 Basic culture methods. Methods Cell. Biol. **48:** 3–29.

L'Hernault, S. W., 1997 Spermatogenesis, pp. 271–294 in *C. Elegans II*, edited by D. L. Riddle, T. Blumenthal, B. J. Meyer and J. R. Priess. Cold Spring Harbor Laboratory Press, Plainview, NY.

L'Hernault, S. W., D. C. Shakes and S. Ward, 1988 Developmental genetics of chromosome I spermatogenesis-defective mutants in the nematode *Caenorhabditis elegans*. Genetics **120:** 435–452.

Machaca, K., L. J. DeFelice and S. W. L'Hernault, 1996 A novel chloride channel localizes to Caenorhabditis elegans spermatids and chloride channel blockers induce spermatid differentiation. Dev. Biol. **176:** 1–16.

Mello, C., and A. Fire, 1995 DNA transformation. Methods Cell Biol. **48:** 451–482.

Miller, S., and E. Myers, 1999 The FAKtory DNA Sequence Fragment Assembly System. Technical Report 99–03, Department of Computer Science, University of Arizona, Tucson, AZ.

Minniti, A. N., C. Sadler and S. Ward, 1996 Genetic and molecular analysis of spe-27, a gene required for spermiogenesis in *Caenorhabditis elegans* hermaphrodites. Genetics **143:** 213–223.

Murakami, A., K. Kimura and A. Nakano, 1999 The inactive form of a yeast casein kinase I suppresses the secretory defect of the sec12 mutant. Implication of negative regulation by the Hrr25 kinase in the vesicle budding from the endoplasmic reticulum. J. Biol. Chem. **274:** 3804–3810.

Nance, J., A. N. Minniti, C. Sadler and S. Ward, 1999 *spe-12* encodes a sperm cell surface protein that promotes spermiogenesis in *Caenorhabditis elegans*. Genetics **152:** 209–220.

Nance, J., E. B. Davis and S. Ward, 2000 *spe-29* encodes a small predicted membrane protein required for the initiation of sperm activation in *Caenorhabditis elegans*. Genetics **156:** 1623–1633.

Nelson, G. A., and S. Ward, 1980 Vesicle fusion, pseudopod extension and amoeboid motility are induced in nematode spermatids by the ionophore monensin. Cell **19:** 457–464.

Plowman, G. D., S. Sudarsanam, J. Bingham, D. Whyte and T. Hunter, 1999 The protein kinases of Caenorhabditis elegans: a model for signal transduction in multicellular organisms. Proc. Natl. Acad. Sci. USA **96:** 13603–13610.

Reinke, V., H. E. Smith, J. Nance, J. Wang, C. Van Doren *et al.*, 2000 A global profile of germline gene expression in C. elegans. Mol. Cell **6:** 605–616.

Riddle, D. L., 1997 *C. elegans II*. Cold Spring Harbor Laboratory Press, Plainview, NY.

Rivers, A., K. F. Gietzen, E. Vielhaber and D. M. Virshup, 1998 Regulation of casein kinase I epsilon and casein kinase I delta by an in vivo futile phosphorylation cycle. J. Biol. Chem. **273:** 15980–15984.

Roberts, T. M., and K. L. King, 1991 Centripetal flow and directed reassembly of the major sperm protein (MSP) cytoskeleton in the amoeboid sperm of the nematode, Ascaris suum. Cell Motil. Cytoskeleton **20:** 228–241.

Roberts, T. M., and M. Stewart, 1995 Nematode sperm locomotion. Curr. Opin. Cell Biol. **7:** 13–17.

Roberts, T. M., and M. Stewart, 2000 Acting like actin. The dynamics of the nematode major sperm protein (msp) cytoskeleton indicate a push-pull mechanism for amoeboid cell motility. J. Cell Biol. **149:** 7–12.

Rowles, J., C. Slaughter, C. Moomaw, J. Hsu and M. H. Cobb, 1991 Purification of casein kinase I and isolation of cDNAs encoding multiple casein kinase I-like enzymes. Proc. Natl. Acad. Sci. USA **88:** 9548–9552.

Shakes, D. C., and S. Ward, 1989 Initiation of spermiogenesis in C. elegans: a pharmacological and genetic analysis. Dev. Biol. **134:** 189–200.

Theriot, J. A., 1996 Worm sperm and advances in cell locomotion. Cell **84:** 1–4.

Varkey, J. P., P. L. Jansma, A. N. Minniti and S. Ward, 1993 The *Caenorhabditis elegans* spe-6 gene is required for major sperm protein assembly and shows second site non-complementation with an unlinked deficiency. Genetics **133:** 79–86.

Ward, S., and J. S. Carrel, 1979 Fertilization and sperm competition in the nematode Caenorhabditis elegans. Dev. Biol. **73:** 304–321.

Ward, S., E. Hogan and G. A. Nelson, 1983 The initiation of spermiogenesis in the nematode Caenorhabditis elegans. Dev. Biol. **98:** 70–79.

Williams, B. D., 1995 Genetic mapping with polymorphic sequence-tagged sites. Methods Cell Biol. **48:** 81–96.

Wood, W. B., 1988 *The Nematode Caenorhabditis elegans*. Cold Spring Harbor Laboratory Press, Cold Spring Harbor, NY.

Zhang, F., A. Strand, D. Robbins, M. H. Cobb and E. J. Goldsmith, 1994 Atomic structure of the MAP kinase ERK2 at 2.3 A resolution. Nature **367:** 704–711.

Communicating editor: P. Anderson